A R C H I V E S O F M E T A L L U R G Y A N D M A T E R I A L S
Volume 58 2013 Issue 3
DOI: 10.2478/amm-2013-0062

J. CZAJA*, J. BERNACZEK*, R. ŚLIWA*

DETERMINATION OF STRESS VALUES BASED ON CALCULATION OF PHOTOELASTIC CONSTANTS ON THE EXAMPLE OF THE SUB-FRAME CONNECTION WITH THE HULL IN A SMALL TRAINING AIRCRAFT

WYZNACZANIE WIELKOŚCI NAPRĘŻEŃ NA PODSTAWIE OBLICZONYCH STAŁYCH ELASTOOPTYCZNYCH NA PRZYKŁADZIE POŁĄCZENIA RAMY SILNIKA Z KADŁUBEM W SAMOLOCIE SZKOLNO-TRENINGOWYM

The above paper presents the example of sub-frame connections with the hull in a small training aircraft and the results of the analysis of a selected connection using the method of reflected light. The connection model was subjected to the loads similar to those existing in a structure using various materials of the connection. Thus, photoelastic deformation image, showing the load applied on the joint was obtained. Then, for the materials used in the model, photoelastic constants were determined, which were used to estimate the stress values in the model. The analysis allowed us to determine the effect of kind and features (mainly hardness) of the used material pads, on mechanical behavior of the elements of joint.
Keywords: photoelastic, reflected light, photoelastic constant, connections, stress

W artykule przedstawiono wyniki analizy wybranego połączenia z wykorzystaniem metody światła odbitego na przykładzie połączenia ramy silnika z kadłubem w małym samolocie szkolno-treningowym, Model połączenia poddano obciążeniom zbliżonym do rzeczywistych występujących w konstrukcji przy zastosowaniu różnych materiałów konstrukcyjnych elementów składowych połączenia. Otrzymano obraz pól odkształceń będący odpowiedzią węzła na zadane obciążenie. Następnie dla materiałów zastosowanych w modelu wyznaczono stałe elastooptyczne, które posłużyły do oszacowania wielkości naprężeń występujących w modelu. Przeprowadzona analiza pozwoliła na określenie wpływu rodzaju i właściwości (głównie twardości) materiału zastosowanej podkładki na zachowanie się pozostałych elementów węzła.

1. Introduction

Structure modeling investigations are the basic tool for an engineer and his work. The knowledge of the structure response to the loads which are applied allows, at the designing stage, the engineers to secure the expected properties of the structure components used in the appliances. It is critical in the case of responsible structures which include aircraft structures, whose inseparable part is a variety of bolt connections [1] [2].

An image of stress and deformation fields, which occur in bolt connections subjected to changeable loads, and which are obtained in the process of modeling, is a crucial factor enabling accurate assessment of the efficiency of the connection work and the effects resulting from it. Determining the row of isochromatics allows showing local stress concentration exceeding many times the flow stress leading to decrease of the connection strength and decrease of the clamping force. Modeling research allows determining the range of necessary changes in the structure and material components of the connection. There are two popular methods of photoelastic research, that is, the reflected light and optically active layer [3] [4] [5] [6].

An important aspect is the assessment of distribution of isochromatics on the surface of the examined component. Although the visible optical effect is not direct flow stress, the isochromatic determines geometrical spot with constant remainder of main stresses σ_1, σ_2 and then it determines directly the value τ_{ekstr}, and then illustrates the level of strain according to the hypothesis of maximum shear stresses.

As by definition isochromatics are curves along which the maximum shear stress is constant, thus, the isochromatics images allow determining the distribution of maximum shear stresses τ_{max} in the examined area of the model on the basis of dependence resulting from Wertheim law:

$$\sigma_1 - \sigma_2 = m K_{\sigma m} \tag{1}$$

then

$$\tau_{\max} = \frac{m}{c} \tag{2}$$

where: m – row of isochromatics determines the value of relative displacement of components of the crossing radius in relation to the full phase angle equal to 2π

$$c = \frac{2}{K_{\sigma m}} \tag{3}$$

* RZESZOW UNIVERSITY OF TECHNOLOGY, POLAND

$K_{\sigma m}$– model photoelastic constant, defining the value of isochromatics row in [MPa]. The above formula implies that the only variable is the row of isochromatics m and in order to determine the differences of main stress and/or maximum shear stresses it suffices to take mesurement of the row of isochromatics.

2. Determination of the photoelastic constant of deformation transformations K (Kε)

Determination of the photoelastic constant of deformation transformations K (Kε) for optically active materials is crucial for proper assessment of the level of deformation or stress in the examined object. Photoelastic constants are provided by material manufacturers [9], however, determination of these constants with the use of appropriately prepared samples and equipment allows determining real properties of the material which is used to manufacture the hull.

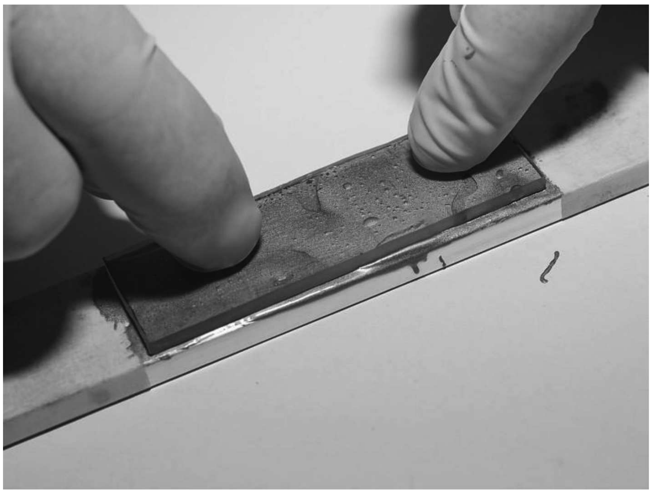

Fig. 1. A sample preparation

The tested sample, after proper preparation of optically active layer, was glued to the measuring beam and then placed in a calibration device – 010 model (Fig. 2)

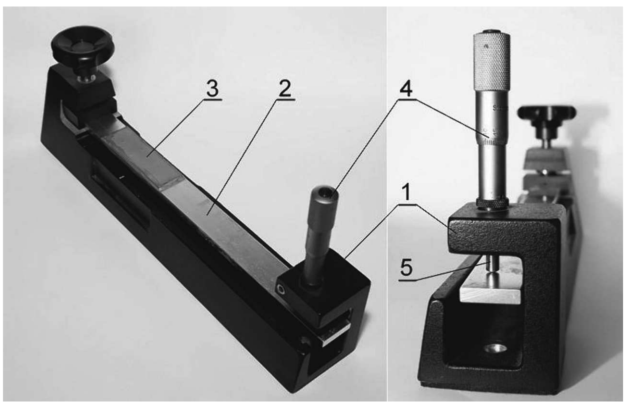

Fig. 2. Device for determination of deformation factor Kε 1- calibration device housing, 2 – measuring beam, 3 - optically active layer, 4 – micrometer, 5 - mandrel

Then the row of isochromatics values were measured in the measuring point for 5 locations of the mandrel displacing axially. Constant values of axial pin displacement were measured by a micrometer. Precise values of the row of isochromatics were measured with the use of a compensator (Table 1). Distribution of isochromatics in the sample of optically active layer (example) is shown in Fig. 3

TABLE 1

Rows of isochromatics depend on mandrel displacement

Item No.	Mandrel displacement D [mm]	Row of isochromatics value N
1	2.5	0.35
2	5	0.80
3	7.5	1.27
4	10	1.74
5	12.5	2,20

Fig. 3. Distribution of isochromatics in the sample of optically active layer

The photoelastic deformation constant may be calculated on the following formula:

$$K_{\Xi} = K' \left[1 + \frac{2\left(t'_A - t_A\right)}{t_B + t_C} \right] \tag{4}$$

Where:

K' – photoelastic deformation constant read from the diagram ([8], fig. 5),

t'_A – standard adhesive thickness (t'_A *=0,075mm),*

t_A– actual adhesive thickness,

t_B– measuring beam thickness (t_B *=6.35mm*),

t_C - optically active layer thickness (t_C *=2.9 mm).*

Constant K' is selected on the basis of ΔN/ΔD value and layer $t_C$thickness.

For value ΔN/ΔD=0,185 and t_C = 2.9mm constant K'= 0.098

The actual adhesive thickness t_A may be calculated by extracting the thickness of layer t_C and measuring beam t_B from the total thickness of measuring beam along with the layer glued.

t_A = 9.35 - 2.9 - 6.35 = 0,15mm

By adding the above values to the formula the actual value of the photoelastic constant of deformation Kε may be calculated.

$$K_\varepsilon = 0.098\left[1 + \frac{2\,(0.075 - 0.150)}{6.35 + 2.9}\right] = 0.0964 \qquad (5)$$

3. Investigation of the sub-frame connection to the hull in a small training aircraft

Connection model shown in Fig. 4a was subjected to the load according to the scheme given in Fig. 4b).

a) b)

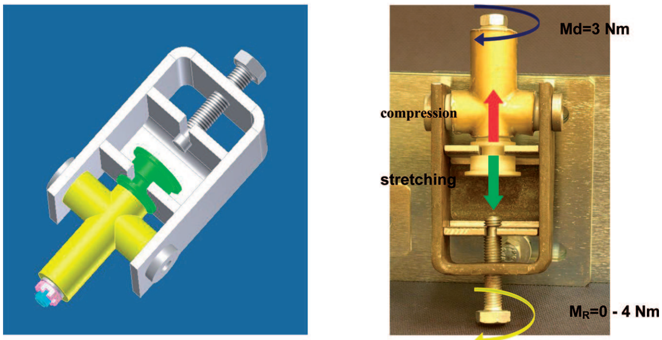

Fig. 4. a) CAD model of a connection tested in the device and b) SLA model with optically active layer in the device

Conducted photoelastic investigation of an aircraft connection illustrates stress distribution in the main sleeve, the effect of the washer and direction used, as well as the amount of the load applied on the stress size.

The tested model, after being covered with optically active material, was furnished in the device. (Fig. 4) The aim of the investigation was to determine the influence of the material used in the connection of the washer on the stress value existing in the main sleeve.

A furnished model was subjected to a load at initial moment equal to Md=3 Nm, and then to additional force acting along bolt axis and turn, resulting in squeezing and stretching the sleeve. A resin washer Full Care 720 and a steel washer were used as substitute components.

Properties of FullCure 720 and steel materials were shown in Table 2.

Table 2. Mechanical properties of resin FullCure 720.

TABLE 2

Properties of FullCure 720 and steel

Feature/property	Unit	FullCure 720	Steel 10
Tensile strength	**MPa**	**60.3**	**410 – 640**
Coefficient of elasticity	**MPa**	**2870**	
Ultimate elongation	%	**20**	**>19**
Hardness		**81 (Rockwell scale M)**	**min. 147 HB**

The investigation was conducted in the device with application of metal washers providing uniform support of the sleeve in the fixture.

The investigation was conducted for the following cases:

1. "Hard" metal washer

– connection squeezed with initial moment 3 Nm and given the following working load:

- compression in the range of: 0 Nm, 2 Nm, 2.5 Nm ... 4 Nm
- stretching in the range of : 1 Nm, 1,5 Nm, 2 Nm ... 3.5 Nm

2. „Soft" washer (resin Jetting Systems – FullCure 720) – connection compressed with initial moment 3 Nm:

- compression in the range of: 0 Nm, 2 Nm, 2.5 Nm ... 4 Nm
- stretching in the range of: 1 Nm, 1,5 Nm, 2 Nm ... 3.5 Nm

The size of the initial moment and the working load was determined with use of a torque spanner equipped with an electronic attachment.

4. The results of photoelastic investigations

Fig. 5-8 demonstrate the received isochromatics images and comparison of value *m* in various cases of loads and various types of washer material.

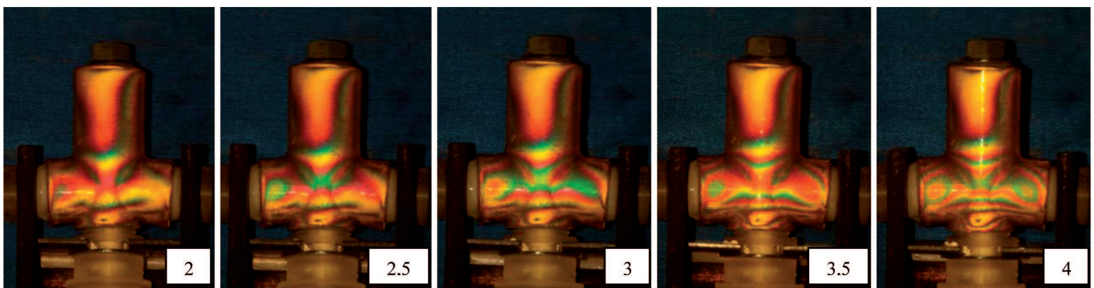

Working load [Nm]	2	2.5	3	3.5	4
Row of izochrom. - *m*	**2**	**2 – 2.5**	**2.5**	**3**	**3.5**

Fig. 5. Isochromatics under the working load from 2 to 4 Nm – connection compressed (force acting upward), steel washer

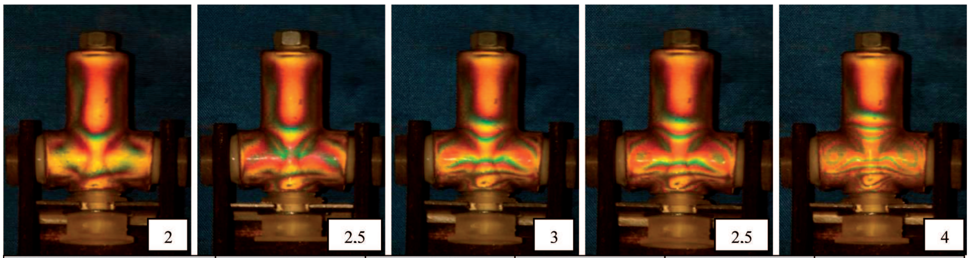

Working load [Nm]	2	2.5	3	3.5	4
Row of izochrom. - *m*	1	2	2.5	3.5	4.5

Fig. 6. Isochromatics under the working load from M=2 to 4 Nm – connection compressed (force acting upward), FullCure 720 washer

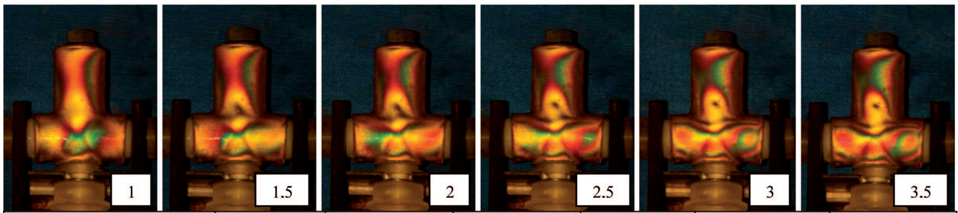

Working load [Nm]	1	1.5	2	2.5	3	3.5
Row of izochrom. - *m*	1	1 – 1.5	1.5	2	2.5	2.5

Fig. 7. Isochromatics under the working load from M=1 to 3,5 Nm – connection stretched (force acting downward), steel washer

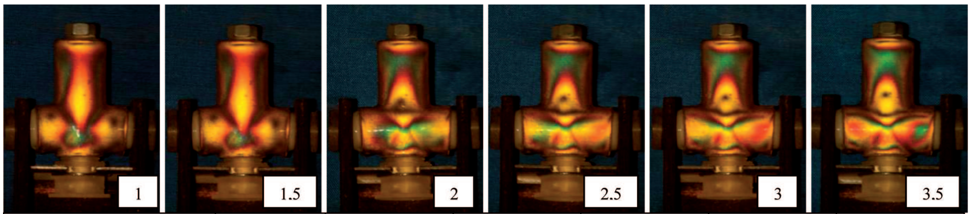

Working load [Nm]	1	1.5	2	2.5	3	3.5
Row of izochrom. - *m*	1	1	1 – 1.5	1.5	1.5	2

Fig. 8. Isochromatics under the working load from M=1 to 3,5 Nm – connection stretched (force acting downward), FullCure 720 washer

Then determined values of the rows of isochromatics were inserted as input data into PSCalc [U+F8E8] Vishay Micro-Measurements program [8 , 9]. Using photoelastic constants determined on a test basis or provided in the specifications of optically active materials along with detailed data of the material used in the modeling process and inserted rows of isochromatics, the program made it possible to calculate stress and deformation values in specified spots of the model.

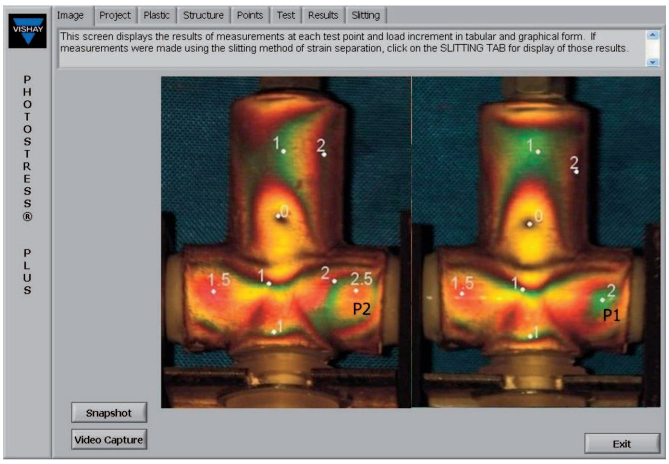

Fig. 9. A sample screen display taken from a camera connected to the test stand. P1, P2 – tested points for which stress and deformation values were determined

Fig. 9 shows a sample screen display taken from a camera connected to the test stand to obtain the input data into the program.

(P1) – FullCure 720 washer model, (P2) – steel washer model

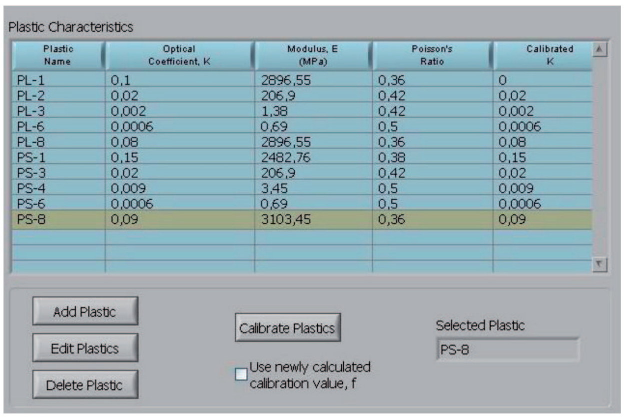

Plastic Name	Optical Coefficient, K	Modulus, E (MPa)	Poisson's Ratio	Calibrated K
PL-1	0,1	2896,55	0,36	0
PL-2	0,02	206,9	0,42	0,02
PL-3	0,002	1,38	0,42	0,002
PL-6	0,0006	0,69	0,5	0,0006
PL-8	0,08	2896,55	0,36	0,08
PS-1	0,15	2482,76	0,38	0,15
PS-3	0,02	206,9	0,42	0,02
PS-4	0,009	3,45	0,5	0,009
PS-6	0,0006	0,69	0,5	0,0006
PS-8	0,09	3103,45	0,36	0,09

Fig. 10. Data on material layer PS-8

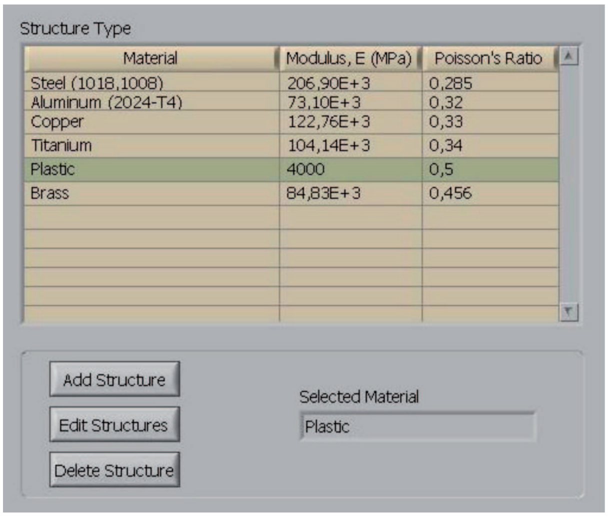

Material	Modulus, E (MPa)	Poisson's Ratio
Steel (1018,1008)	206,90E+3	0,285
Aluminum (2024-T4)	73,10E+3	0,32
Copper	122,76E+3	0,33
Titanium	104,14E+3	0,34
Plastic	4000	0,5
Brass	84,83E+3	0,456

Fig. 11. Data on material of the sleeve model

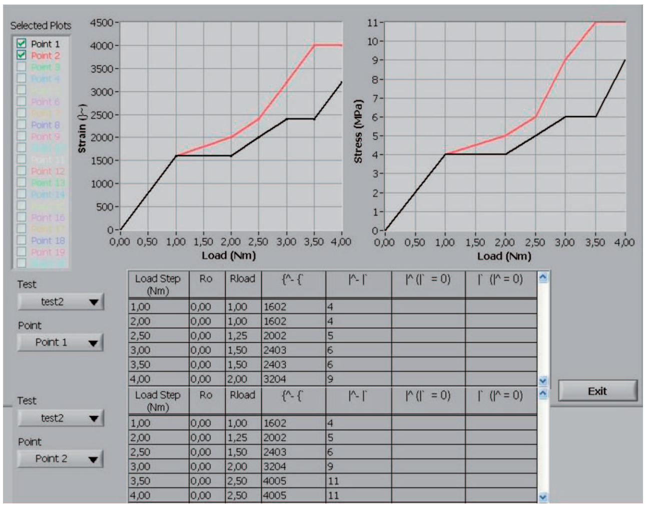

<table>
<tr><th>Load Step (Nm)</th><th>Ro</th><th>Rload</th><th>{^- {`</th><th>|^- |`</th><th>|^ (|` = 0)</th><th>|` (|^ = 0)</th></tr>
<tr><td>1,00</td><td>0,00</td><td>1,00</td><td>1602</td><td>4</td><td></td><td></td></tr>
<tr><td>2,00</td><td>0,00</td><td>1,00</td><td>1602</td><td>4</td><td></td><td></td></tr>
<tr><td>2,50</td><td>0,00</td><td>1,25</td><td>2002</td><td>5</td><td></td><td></td></tr>
<tr><td>3,00</td><td>0,00</td><td>1,50</td><td>2403</td><td>6</td><td></td><td></td></tr>
<tr><td>3,50</td><td>0,00</td><td>1,50</td><td>2403</td><td>6</td><td></td><td></td></tr>
<tr><td>4,00</td><td>0,00</td><td>2,00</td><td>3204</td><td>9</td><td></td><td></td></tr>
</table>

<table>
<tr><th>Load Step (Nm)</th><th>Ro</th><th>Rload</th><th>{^- {`</th><th>|^- |`</th><th>|^ (|` = 0)</th><th>|` (|^ = 0)</th></tr>
<tr><td>1,00</td><td>0,00</td><td>1,00</td><td>1602</td><td>4</td><td></td><td></td></tr>
<tr><td>2,00</td><td>0,00</td><td>1,25</td><td>2002</td><td>5</td><td></td><td></td></tr>
<tr><td>2,50</td><td>0,00</td><td>1,50</td><td>2403</td><td>6</td><td></td><td></td></tr>
<tr><td>3,00</td><td>0,00</td><td>2,00</td><td>3204</td><td>9</td><td></td><td></td></tr>
<tr><td>3,50</td><td>0,00</td><td>2,50</td><td>4005</td><td>11</td><td></td><td></td></tr>
<tr><td>4,00</td><td>0,00</td><td>2,50</td><td>4005</td><td>11</td><td></td><td></td></tr>
</table>

Fig. 12. Calculated values of deformation and stress in P1, P2 spots under the working load moment – force direction – stretching

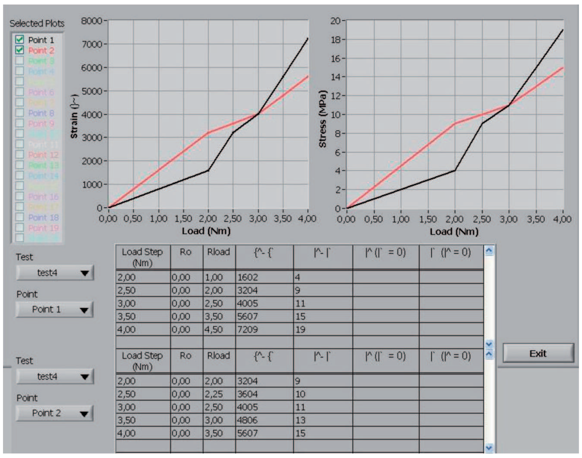

<table>
<tr><th>Load Step (Nm)</th><th>Ro</th><th>Rload</th><th>{^- {`</th><th>|^- |`</th><th>|^ (|` = 0)</th><th>|` (|^ = 0)</th></tr>
<tr><td>2,00</td><td>0,00</td><td>1,00</td><td>1602</td><td>4</td><td></td><td></td></tr>
<tr><td>2,50</td><td>0,00</td><td>2,00</td><td>3204</td><td>9</td><td></td><td></td></tr>
<tr><td>3,00</td><td>0,00</td><td>2,50</td><td>4005</td><td>11</td><td></td><td></td></tr>
<tr><td>3,50</td><td>0,00</td><td>3,50</td><td>5607</td><td>15</td><td></td><td></td></tr>
<tr><td>4,00</td><td>0,00</td><td>4,50</td><td>7209</td><td>19</td><td></td><td></td></tr>
</table>

<table>
<tr><th>Load Step (Nm)</th><th>Ro</th><th>Rload</th><th>{^- {`</th><th>|^- |`</th><th>|^ (|` = 0)</th><th>|` (|^ = 0)</th></tr>
<tr><td>2,00</td><td>0,00</td><td>2,00</td><td>3204</td><td>9</td><td></td><td></td></tr>
<tr><td>2,50</td><td>0,00</td><td>2,25</td><td>3604</td><td>10</td><td></td><td></td></tr>
<tr><td>3,00</td><td>0,00</td><td>2,50</td><td>4005</td><td>11</td><td></td><td></td></tr>
<tr><td>3,50</td><td>0,00</td><td>3,00</td><td>4806</td><td>13</td><td></td><td></td></tr>
<tr><td>4,00</td><td>0,00</td><td>3,50</td><td>5607</td><td>15</td><td></td><td></td></tr>
</table>

Fig. 13. Calculated values of deformation and stress-in P1, P2 spots under the working load moment – force direction – compressing

Additionally, having photoelastic constants determined on a test basis, one may determine approximate distribution of stress values existing in the examined model. Fig. 14-17 demonstrate stress fields in selected cases of direction, working load size and washer material.

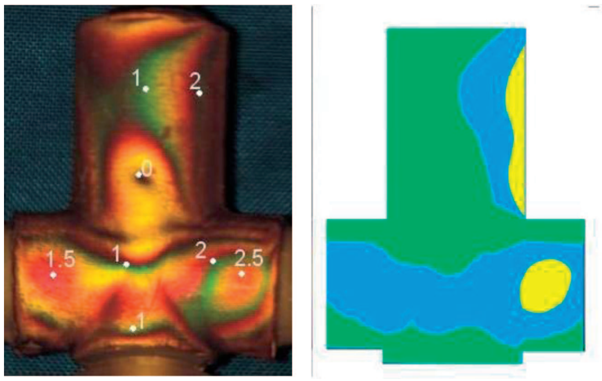

Fig. 14. Stress distribution: working load = 3,5 Nm, steel washer, stretching

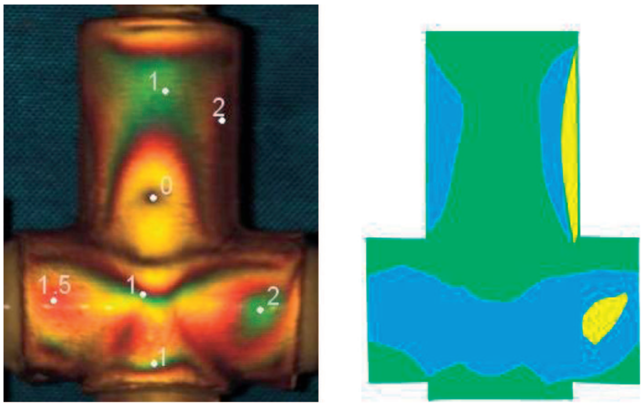

Fig. 15. Stress distribution: working load = 3,5 Nm, FullCure 720 washer, stretching

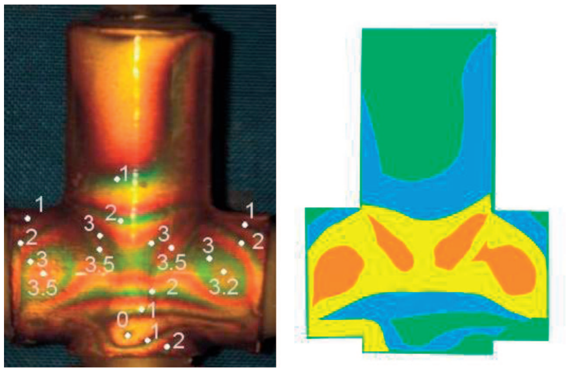

Fig. 16. Stress distribution: working load = 4,0 Nm, steel washer, compressing

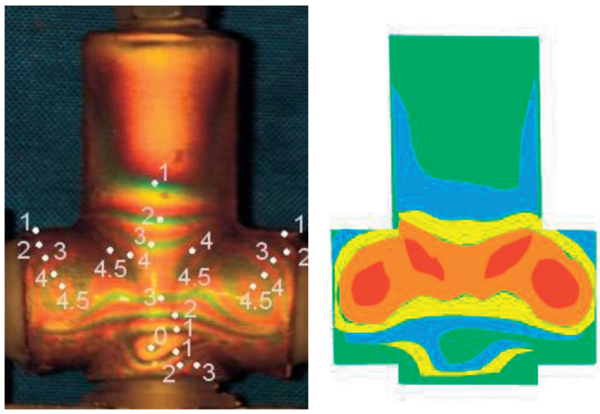

Fig. 17. Stress distribution: working load = 4 Nm, FullCure 720 washer, compressing

5. Conclusions

1. The achieved results show various stress values in the sleeve depending on the type of washer material and force direction (fig 12, 13). In case of stretching, a soft washer causes smaller stresses in the sleeve than a hard washer. The 'absorbing' properties of the washer are proved. In case of squeezing, the application of a soft washer causes increase of the row of isochromatics proving an increase of stress values in the sleeve. Application of a hard washer decreases the row of isochromatics by one and the growth of the rows of isochromatics is smaller. The sleeve structure itself may have an effect on the observed changes, where the distance of clamping arms from the sleeve ends is not equal.
2. Stress distribution shown in figures 14-17 illustrates roughly stress values existing in particular areas. It results from lack of possibility to determine the row of isochromatics accurately, especially in the areas of solid model refraction but also lack of possibility to determine the boundaries of particular rows of isochromatics areas. Application of specialist imaging software/equipment would make it possible to eliminate mistakes occurring while determining these areas, and what is more, increase the investigation accuracy.
3. Application of photelastic methods (reflected or reflective light) in the investigations of structural components allows determining potentially vulnerable areas and estimating the deformation and stress values existing in the structure.
4. The knowledge of photoelastic constants determined on the basis of test samples made it possible to assess the deformation and stress level in particular areas of the connection of the sub-frame and the hull in a small training aircraft.

Received: 20 November 2013.

Acknowledgements

Financial support of Structural Funds in the Operational Programme – Innovative Economy (IE OP) financed from the European Regional Development Fund – Project "Modern material technologies in aerospace industry", No POIG.0101.02-00-015/08 is gratefully acknowledged.

REFERENCES

[1] N. Eliaz, G. Gheorghiu, H. Sheinkopf, O. Levi, G. Shemesh, A. Ben-Mordechai, H. Artzi, Failures of bolts in helicopter main rotor drive plate assembly due to improper application of lubricant , Engineering Failure Analysis **10**(4), 443-451 (2003).

[2] K.W. Olsen, Fatigue crack growth analyses and experimental verification of aerospace threaded fasteners; Department of Mechanical and Aerospace Engineering; Case Western Reserve University; 2004.

[3] R.S. Doroszkiewicz, Elastooptyka. Stan i rozwój polaryzacyjno-optycznych metod doświadczalnej analizy naprężeń. Polska Akademia Nauk, Instytut Podstawowych Problemów Techniki, PWN, Warszawa – Poznań 1975.

[4] H. Kopecki, Problemy analizy stanów naprężenia ustrojów w świetle badań eksperymentalnych metodami mechaniki modelowej. Zeszyty Naukowe Politechniki Rzeszowskiej, nr 78, Mechanika, z. 26, Rzeszów 1992.

[5] M. Kopkowicz, Metody doświadczalne badań konstrukcji. Oficyna Wydawnicza Politechniki Rzeszowskiej, Rzeszów 2003.

[6] J.T. Pindera, Zarys elastooptyki. PWT, Warszawa 1953.

[7] TN – 701-1. Vishay Precision Group.

[8] PhotoStress Analysis Systems. Installation Guide – Vishay Precision Group.

[9] 11222. Vishay Precision Group.